Extreme Ultraviolet Fourier-Transform Spectroscopy with High Order Harmonics

M. Kovačev,[1] S. V. Fomichev,[2] E. Priori,[3] Y. Mairesse,[1] H. Merdji,[1] P. Monchicourt,[1] P. Breger,[1] J. Norin,[4] A. Persson,[4] A. L'Huillier,[4] C.-G. Wahlström,[4] B. Carré,[1] and P. Salières[1]

[1]*CEA/DSM/DRECAM/SPAM, bât. 522, Centre d'Etudes de Saclay, 91191 Gif-sur-Yvette, France*
[2]*Institute of Molecular Physics, RRC "Kurchatov Institute", 123182 Moscow, Russia*
[3]*INFM, Dipartimento di Fisica, Politecnico di Milano, 20133 Milano, Italy*
[4]*Department of Physics, Lund Institute of Technology, P.O. Box 118, S-221 00 Lund, Sweden*

(Received 22 July 2005; published 23 November 2005)

We demonstrate a new scheme for extreme ultraviolet (xuv) Fourier-transform spectroscopy based on the generation of two phase-locked high-harmonic beams. It allows us to measure for the first time interferograms at wavelengths as short as 90 nm, and open the perspective of performing high-resolution Fourier-transform absorption spectroscopy in the xuv. Our measurements also demonstrate that a precise control of the relative phase of harmonic pulses can be obtained with an accuracy on an attosecond time scale, of importance for future xuv pump-xuv probe attosecond spectroscopy.

DOI: 10.1103/PhysRevLett.95.223903 PACS numbers: 42.65.Ky, 42.65.Re, 42.87.Bg

Fourier-transform spectroscopy (FTS) is a widely used technique in the infrared, visible, and ultraviolet ranges [1,2]. This is due to both its wavelength accuracy and its extremely high resolution, only limited by the length and stability of the delay line, that can surpass that of the best grating spectrometers. Unfortunately few attempts have been made to extend this technique to the extreme ultraviolet (xuv) range [3], because many difficulties arise in this demanding spectral domain. First, the beam to characterize has to be split in two replicas. Since xuv beam splitters did not exist until recently (good optical elements with small absorption are still a challenge) [4,5], wave front division of a spatially coherent beam was proposed [6,7]. Second, the delay between the two replicas must be precisely controlled and varied on the time scale of the xuv optical period, i.e., on an attosecond time scale: the stability and resolution of the delay line must be on a nanometer length scale, which is challenging in a lab environment. Finally, the beams should be combined in order that they interfere, which raises the problem of the combining element. The signal *oscillating as a function of the delay* [or optical path difference (OPD)] is a first-order autocorrelation (or interferogram) of the incoming beam. Its Fourier transform gives the power spectrum of the radiation. The scaling of both optical and mechanical tolerances with the wavelength, together with the strong absorption in the xuv range, are thus the main reasons for the absence of FTS data at wavelengths below 130 nm.

An elegant way to produce replicas (first requirement) is to generate two mutually coherent xuv beams, without need of splitting. This has recently become possible thanks to the generation of high harmonics (HHG) of intense laser pulses [8]. Two space-separated, usually undelayed, phase-locked harmonic pulses can be generated from two replicas of the laser pulse focused at two different locations in a rare gas jet [9]. In this scheme, the two beams combine in the far field by natural diffraction and produce an interference pattern similar to the Young's double slit fringes. Similarly, two time-separated, spatially superposed, phase-locked harmonic pulses are generated from two time-delayed laser pulses focused at the same location [10,11]. This scheme allows frequency-domain interferometry. Both techniques have been applied to plasma diagnostic using xuv interferometry [10,12]. The time-separation method has been used to perform Ramsey-fringe spectroscopy [13,14] or to generate a frequency comb [15,16]. However, none of the two methods in their initial form is adapted to FTS. Spectral measurement of harmonics has been reported in a scheme related to space separation, but under assumption of spatial coherence [17]. In the time-separation scheme, the intrinsic nonlinearity of HHG does not allow overlapping the two pulses in time without strongly distorting them. In contrast, the combination of a space and a variable time separation makes FTS possible. In a first step, by sampling the contrast of the far-field fringes at different delays, one has access to the coherence time [18,19]. Now, by continuously monitoring the variation of the fringe pattern as a function of the delay, one should measure the harmonic first-order autocorrelation. One therefore accesses to both the absolute wavelength and the line shape of the xuv light.

In this Letter, we demonstrate xuv Fourier-transform spectroscopy of high-order harmonics in the space- and time-separation scheme. Our interferometric setup does not rely on any xuv optics, but on an infrared Michelson-type setup, and would allow performing broadband absorption spectroscopy of a target gas. To our knowledge, we measure for the first time interferograms at wavelengths as short as 90 nm, corresponding to harmonic 9. We study in detail the influence of the separation between the two laser foci, and observe a transition from a first-order autocorrelation of the harmonic beam to a high-order autocorrelation

of the laser beam. Measurements show good agreement with simulations of interferometric traces including both the single-atom response and the beam propagation.

In our experimental setup, shown in Fig. 1, an intense infrared (IR) pulse from the 810 nm, 80 mJ, 60 fs LUCA laser is sent in a Michelson-type interferometer that produces two time-delayed IR pulses. By slightly misaligning one arm, the two pulses can be focused at different locations (separated by distance d) in a 90 Torr xenon jet, generating two phase-locked harmonic sources. The laser intensity in each focus reaches 10^{14} W/cm^2, and the waist is 100 μm. We then filter out the strong fundamental radiation, either with a low-resolution grating monochromator for observing one single harmonic, or with an aluminum filter (1000 Å) for transmitting the full spectrum above harmonic 11. After diffraction, the two harmonic beams produce an interference pattern that is recorded on a 2D detector [dual microchannel plates (MCP) coupled to a phosphor screen and a CCD camera] placed 1 m after the image plane of the toroidal mirror. The MCP were CsI-coated to intensify their response in the xuv and had a spatial resolution of 80 μm. By integrating the signal inside a narrow window (whose width is a fraction of a fringe) positioned at the center of the far-field profile, we measure the interference between equivalent rays in the two xuv beams. The signal of harmonic q can be written:

$$S_q^1(\tau) = \int_{-\infty}^{+\infty} |E_q(t) + E_q(t-\tau)|^2 dt, \qquad (1)$$

where E_q is the harmonic electric field. When scanning the delay τ between the IR pulses, i.e., between the harmonic pulses, the xuv intensity in the integrating window is periodically modulated (the total energy does not change). A first-order autocorrelation of the harmonic beam is thus recorded, provided that a high enough stability and resolution are achieved on the delay line. Two independent translation stages were used: a long-range stage (25 mm) with micrometer accuracy to find the zero OPD and a short-range piezoelectric stage (90 μm) with nanometer accuracy to provide the fine OPD tuning. The accurate positioning of the latter is ensured by a capacitive measurement system and a position control module (Piezo-Systems-Jena). The stability of the Michelson is a key issue: in order to measure the interferogram of, e.g., harmonic 9 ($\lambda = 89$ nm), the relative vibrational amplitude of the interferometer's optical elements must be less than $\sim$10 nm. This is of the same order as the seismic background and far below the disturbances in the lab environment. Besides a robust construction and passive vibration isolation, the interferometer was placed in a vacuum chamber to isolate from heat, air turbulence, and noise.

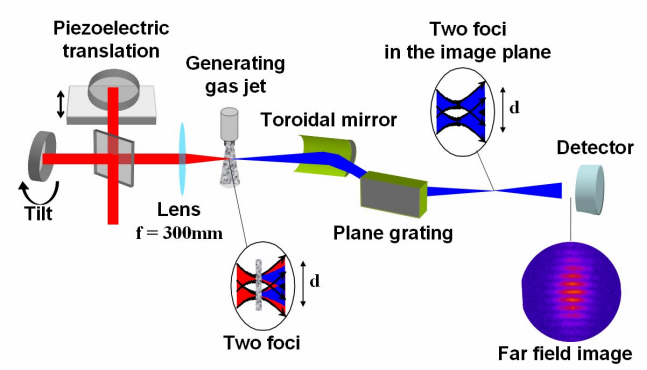

FIG. 1 (color online). Experimental setup for the Fourier-transform spectroscopy of high harmonics.

A crucial question for realizing the above FTS scheme is: how separated must the two laser foci be in order to generate two "independent" harmonic sources? We first show in Fig. 2(a) the trace obtained for two overlapping laser foci. The 9th harmonic signal shows pronounced oscillations at the laser optical period. In contrast to the FTS scheme, these oscillations are due to the modulation of the total radiated harmonic energy. Indeed, two IR laser beams interfere in the generating medium, which modulates the total laser intensity and consequently the harmonic production. Trace 2(a) is thus a high-order autocorrelation of the IR laser pulse [20]:

$$S_q^p(\tau) = \int_{-\infty}^{+\infty} |E_L(t) + E_L(t-\tau)|^{2p} dt, \qquad (2)$$

where E_L is the laser electric field, and p the effective order of nonlinearity. Since we are not in a perturbative regime, p is much smaller than the harmonic order q [21]. Frequency spectrum of trace 2(a) (FT) is plotted in Fig. 2(b). It exhibits a peak at the laser frequency and rapidly decreasing harmonic peaks, corresponding to the decomposition of a quasiperiodic function into its discrete frequency components. Note that there is no detectable signal at the 9th harmonic. In order to measure the first-order autocorrelation of the harmonic beam, we now separate the two laser foci by slightly tilting one mirror in the interferometer. The

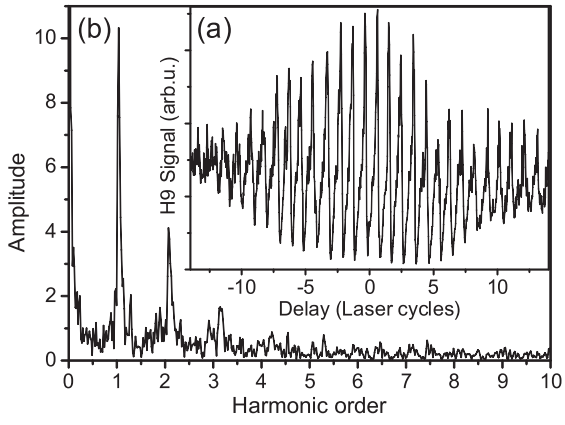

FIG. 2. (a) Experimental trace obtained for the 9th harmonic generated by two collinear laser pulses ($d = 0$). (b) Fourier transform of the trace.

influence of this separation is shown in Fig. 3. For partially separated laser beams ($d \approx 90$ μm is of the order of the laser waist), the trace is still strongly modulated at the laser period, but shows the onset of oscillations at the 9th harmonic [Figs. 3(a) and 3(b)]. At intermediate separation ($d \approx 135$ μm), the trace exhibits pronounced harmonic oscillations over almost the full observation range. Finally, at maximum separation ($d \approx 300$ μm), the laser frequency modulation is strongly reduced [Figs. 3(e) and 3(f)]; the period of the far-field fringes is very small, which means that signal is reduced and more sensitive to vibrations. In all these traces, we performed a very fine sampling to demonstrate the high accuracy and stability of our setup: a harmonic period (300 as) is sampled with 10 points (1 point every 33 as). The clear oscillations in the zooms of Fig. 3 demonstrate the accurate control of the relative phase of the harmonic pulses on an attosecond time scale. This will be crucial for performing attosecond xuv pump-xuv probe spectroscopy [22]. Note that the acquisition time for each trace was about 2 h (at 20 Hz laser rep rate), which demonstrates the long term stability of the setup. The Fourier transforms of the experimental traces are shown in Figs. 4(a), 4(c), and 4(e). The large peak at the fundamental frequency progressively declines while the harmonic peak grows, and the sideband peaks disappear. We thus observe a progressive transition from a high-order autocorrelation of the fundamental beam to a first-order autocorrelation of the high-harmonic beam.

In order to validate our measurements, we have performed systematic simulations of the interferometric traces in the experimental conditions [23]. The distribution of nonlinear atomic dipole in the total driving field (sum of the two fields separately focussed) is calculated in the strong-field approximation (SFA) [24]. The macroscopic xuv field is obtained from the propagation equations, taking into account linear and nonlinear atomic dispersion, ionization of the medium [under Ammosov-Delone-Krainov theory [25]], and electronic dispersion. Note that, due to the absence of axial symmetry in the two-foci geometry, a full 3D simulation is required in principle. On the other hand, the accurate calculation of the interferometric traces requires a fine sampling of the delay between the two laser pulses. To limit the calculation time, we thus use a 2D model neglecting the spatial dimension perpendicular to the plane of the two laser beams, as unrelated to the interference effect. The Fourier transforms of the simulated traces are plotted in Figs. 4(b), 4(d), and 4(f). They show qualitatively the same evolution with increasing source separation as the experimental curves. The trace simulated for maximum beam separation of 300 μm was compared to the first-order autocorrelation of the harmonic beam generated by a single laser beam, and is indeed exactly the same, so that its Fourier transform shown in Fig. 4(f) is really the power spectrum of each harmonic beam, as would be obtained with a conventional (high-resolution) spectrometer. The inset in Fig. 4 shows the good agreement between the experimental and simulated H9 spectra of Figs. 4(e) and 4(f). An interesting

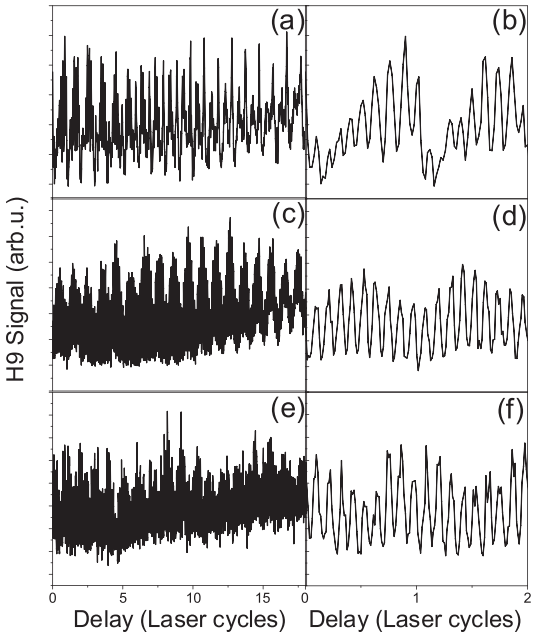

FIG. 3. Experimental traces of the 9th harmonic (left panels) and corresponding zooms of the first two laser periods (right panels), for different values of the laser foci separation d: (a), (b) $d \approx 90$ μm, (c), (d) $d \approx 135$ μm, (e), (f) $d \approx 300$ μm.

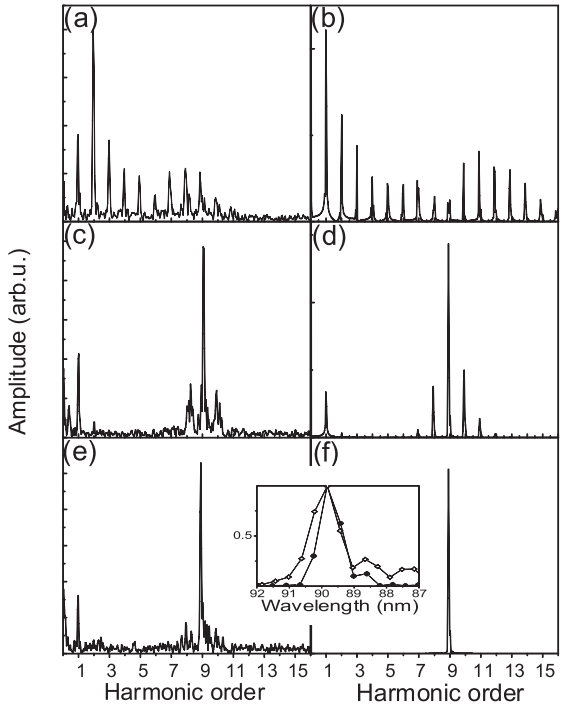

FIG. 4. (a), (c), (e) Fourier transforms of the experimental traces presented in Fig. 3. (b), (d), (f) Fourier transforms of the corresponding simulated traces. The inset shows enlarged H9 spectra of (e) (white circles) and (f) (black dots).

situation arises at the intermediate separation of $d \approx 135\ \mu$m [Figs. 4(c) and 4(d)], with the appearance of sidebands at even harmonic frequencies 8 and 10: these sidebands result from a modulation, at the laser period, of the harmonic electric field. This is an intermediate situation between Eqs. (1) and (2) with a mixing between first-order autocorrelation of the harmonic beam and high-order autocorrelation of the laser beam.

By setting the grating in the zeroth order and using an aluminum filter, our setup allows performing a broadband spectral measurement. The interferogram then exhibits a beating pattern with the periodicity of a half laser cycle. The corresponding spectrum contains the contribution of the experimentally selected harmonic orders (H11 to H17). By placing a target gas jet in the image plane of the toroidal mirror (see Fig. 1), our setup has the potential for Fourier-transform absorption spectroscopy in the gas phase. The close enough locations of the harmonic beams ensure that they probe the same target. Today, structure and energetics of atoms and molecules [26,27], ions, and reactive species (radicals) [28] are priorily investigated in high-resolution xuv spectroscopy, both on narrow band lasers and on incoherent broadband sources such as synchrotron radiation. Moreover, time-resolved spectroscopy should become a key tool for studying dynamics in photochemistry: after pump pulse triggers the reaction, transient intermediate is probed in absorption. In such pump/probe scheme, femtosecond resolution requires *broadband* and *coherent* xuv pulses, the spectral resolution being appropriately adapted. To that goal, the proposed FTS scheme using ultrashort harmonics should be particularly suitable. The large number of photons [$>10^{11}$ per harmonic pulse [29]] and short pulse duration [a few 10 fs [30]] as compared to the picosecond regime [31] allow to probe highly dilute transient species. Moreover, the xuv probe pulse is naturally synchronized with the generating laser beam that can provide the pump pulse. In our experiment, the resolving power was limited to 2×10^3 both by the piezotranslation range (90 μm) and by the long acquisition time at 20 Hz laser rep rate. With the currently available 1 kHz lasers, and using external indexation of the position allowing an OPD of 1 cm [6], a resolving power of 2×10^5 at 90 nm could be achieved.

In conclusion, we have demonstrated the feasibility of xuv Fourier-transform spectroscopy based on the generation of two phase-locked harmonic beams. This scheme does not rely on xuv optics and can cover a large spectral range (many 10 eV) with a high accuracy. Thanks to the intense ultrashort pulses, it has the potential for time-resolved spectroscopy on short-lived transient species with a pump-probe setup. We therefore believe that such a system will be an important tool for the development of xuv high-resolution Fourier-transform spectroscopic applications.

We thank D. Joyeux for illuminating discussions. S. F. acknowledges support from the FEMTO program of the ESF. This work was partially supported by the Swedish Science Council and the European Community under Contracts No. MCRTN-CT-2003-505138 and No. ERB-FMGE-CT950020 (DG12).

[1] J. Chamberlain, *The Principles of Interferometric Spectroscopy* (Wiley, New York, 1979).
[2] A. Cheung *et al.*, J. Chem. Phys. **119**, 8373 (2003).
[3] M. R. Howells *et al.*, Nucl. Instrum. Methods Phys. Res., Sect. A **347**, 182 (1994).
[4] L. B. DaSilva *et al.*, Appl. Opt. **34**, 6389 (1995).
[5] R. F. Smith *et al.*, Opt. Lett. **28**, 2261 (2003).
[6] N. De Oliveira *et al.*, Surf. Rev. Lett. **9**, 655 (2002).
[7] D. Joyeux *et al.*, in *FTS/HISE Topical Meetings on CD-ROM*, FWA1 (The Optical Society of America, Washington, DC, 2005).
[8] P. Salières *et al.*, Adv. At. Mol. Opt. Phys. **41**, 83 (1999).
[9] R. Zerne *et al.*, Phys. Rev. Lett. **79**, 1006 (1997).
[10] P. Salières *et al.*, Phys. Rev. Lett. **83**, 5483 (1999).
[11] M. Bellini *et al.*, Opt. Lett. **26**, 1010 (2001).
[12] D. Descamps *et al.*, Opt. Lett. **25**, 135 (2000).
[13] S. Cavalieri, R. Eramo, M. Materazzi, C. Corsi, and M. Bellini, Phys. Rev. Lett. **89**, 133002 (2002).
[14] S. Witte *et al.*, Science **307**, 400 (2005).
[15] R. J. Jones, K. D. Moll, M. J. Thorpe, and J. Ye, Phys. Rev. Lett. **94**, 193201 (2005).
[16] C. Gohle *et al.*, Nature (London) **436**, 234 (2005).
[17] R. A. Bartels *et al.*, Opt. Lett. **27**, 707 (2002).
[18] M. Bellini *et al.*, Phys. Rev. Lett. **81**, 297 (1998).
[19] C. Lynga *et al.*, Phys. Rev. A **60**, 4823 (1999).
[20] N. A. Papadogiannis, E. Hertz, C. Kalpouzos, and D. Charalambidis, Phys. Rev. A **66**, 025803 (2002).
[21] C. G. Wahlström *et al.*, Phys. Rev. A **48**, 4709 (1993).
[22] P. Tzallas *et al.*, Nature (London) **426**, 267 (2003).
[23] In the simulation, a 90 fs laser pulse is focussed 3.5 mm after a 3 mm xenon jet. The other parameters are indicated in the text.
[24] M. Lewenstein, Ph. Balcou, M. Yu. Ivanov, A. L'Huillier, and P. B. Corkum, Phys. Rev. A **49**, 2117 (1994).
[25] A. M. Perelomov *et al.*, Sov. Phys. JETP **23**, 924 (1966); M. V. Ammosov *et al.*, Sov. Phys. JETP **64**, 1191 (1986).
[26] A. Osterwalder *et al.*, J. Chem. Phys. **121**, 11 810 (2004).
[27] S. Willitsch *et al.*, J. Chem. Phys. **120**, 1761 (2004).
[28] T. Schüssler *et al.*, Phys. Chem. Chem. Phys. **7**, 819 (2005).
[29] J.-F. Hergott *et al.*, Phys. Rev. A **66**, 021801(R) (2002).
[30] A. Bouhal *et al.*, Phys. Rev. A **58**, 389 (1998).
[31] F. Brandi, D. Neshev, and W. Ubachs, Phys. Rev. Lett. **91**, 163901 (2003).